

An Assessment of Subseasonal Prediction Skill of the Antarctic Sea Ice Edge



Key Points:

- A single dynamical system provides probabilistic estimates of the Antarctic sea ice edge, skillful for up to 38 days
- The best multi-model forecast skillfully predicts the Antarctic sea ice edge up to 60 days in advance
- The probabilistic sea ice edge prediction skill depends on sea ice initialization, system physics, and ensemble size

Correspondence to:

Y. Nie,
nieyafei@sml-zhuhai.cn

Citation:

Gao, Y., Xiu, Y., Nie, Y., Luo, H., Yang, Q., Zampieri, L., et al. (2024). An assessment of subseasonal prediction skill of the Antarctic sea ice edge. *Journal of Geophysical Research: Oceans*, 129, e2024JC021499. <https://doi.org/10.1029/2024JC021499>

Received 24 JUN 2024

Accepted 6 NOV 2024

Author Contributions:

Conceptualization: Yafei Nie, Qinghua Yang, Lorenzo Zampieri, Petteri Uotila

Data curation: Yuchun Gao

Formal analysis: Yuchun Gao, Hao Luo, Lorenzo Zampieri, Xianqing Lv

Funding acquisition: Yafei Nie, Qinghua Yang

Investigation: Yuchun Gao, Yongwu Xiu, Petteri Uotila

Methodology: Yuchun Gao, Yongwu Xiu, Hao Luo, Lorenzo Zampieri

Supervision: Yafei Nie, Petteri Uotila

Validation: Yuchun Gao, Yongwu Xiu, Yafei Nie, Hao Luo, Qinghua Yang, Petteri Uotila

Visualization: Yuchun Gao, Xianqing Lv

Writing – original draft: Yuchun Gao, Yongwu Xiu, Yafei Nie, Hao Luo, Qinghua Yang, Petteri Uotila

Yuchun Gao^{1,2}, Yongwu Xiu^{3,4}, Yafei Nie³, Hao Luo³, Qinghua Yang³, Lorenzo Zampieri⁵, Xianqing Lv^{1,2}, and Petteri Uotila⁶

¹Frontier Science Center for Deep Ocean Multispheres and Earth System (FDOMES) and Physical Oceanography Laboratory, Ocean University of China, Qingdao, China, ²Laboratory for Ocean Dynamics and Climate, Qingdao Marine Science and Technology Center, Qingdao, China, ³School of Atmospheric Sciences, Sun Yat-Sen University, and Southern Marine Science and Engineering Guangdong Laboratory (Zhuhai), Zhuhai, China, ⁴Nansen Environmental and Remote Sensing Center, Bergen, Norway, ⁵CMCC Foundation—Euro-Mediterranean Center on Climate Change, Bologna, Italy, ⁶Institute for Atmospheric and Earth System Research/ Physics, Faculty of Science, University of Helsinki, Helsinki, Finland

Abstract In this study, the subseasonal Antarctic sea ice edge prediction skill of the Copernicus Climate Change Service (C3S) and Subseasonal to Seasonal (S2S) projects was evaluated by a probabilistic metric, the spatial probability score (SPS). Both projects provide subseasonal to seasonal scale forecasts of multiple coupled dynamical systems. We found that predictions by individual dynamical systems remain skillful for up to 38 days (i.e., the ECMWF system). Regionally, dynamical systems are better at predicting the sea ice edge in the West Antarctic than in the East Antarctic. However, the seasonal variations of the prediction skill are partly system-dependent as some systems have a freezing-season bias, some had a melting-season bias, and some had a season-independent bias. Further analysis reveals that the model initialization is the crucial prerequisite for skillful subseasonal sea ice prediction. For those systems with the most realistic initialization, the model physics dictates the propagation of initialization errors and, consequently, the temporal length of predictive skill. Additionally, we found that the SPS-characterized prediction skill could be improved by increasing the ensemble size to gain a more realistic ensemble spread. Based on the C3S systems, we constructed a multi-model forecast from the above principles. This forecast consistently demonstrated a superior prediction skill compared to individual dynamical systems or statistical observation-based benchmarks. In summary, our results elucidate the most important factors (i.e., the model initialization and the model physics) affecting the currently available subseasonal Antarctic sea ice prediction systems and highlighting the opportunities to improve them significantly.

Plain Language Summary Dynamical atmosphere-ocean prediction systems providing multi-scale temporally wide-ranging sea ice forecasts are handy tools for making consistent short-term predictions. Subseasonal Antarctic sea ice forecasts (from two to 8 weeks) could provide practical guidance for research, navigation, ecosystem services, and the blue economy. For this reason, we evaluated the sea ice edge forecasts from two projects (C3S and S2S) and found that one single system could make compelling predictions up to 38 days in advance. Moreover, the prediction skill was higher in the West Antarctic than in the East Antarctic, whereas the seasonal variation of the prediction skill was system dependent. We also found that the prediction performance of the dynamical system is primarily influenced by the sea ice initialization, then by the model physics and the number of simulations included in one system. Based on the above factors, we produced a forecast, based on a combination of different systems that could predict the Antarctic sea ice edge location more than 60 days in advance. This work could be continued by exploring atmosphere-ice-ocean interaction-related processes to improve prediction skills further and better understand Antarctic sea ice's evolution.

1. Introduction

The Antarctic sea ice plays a crucial role in Earth's climate system. Its freezing, melting, and transport not only impact atmospheric and oceanic circulation (Bader et al., 2013; Haumann et al., 2016; Zhang et al., 2024) and marine ecosystems (Jenouvrier et al., 2014) but also place constraints on human activities such as fisheries, tourism, and scientific expeditions in the Southern Ocean. Since August 2016, there has been a dramatic reduction in Antarctic sea ice extent (SIE) accompanied by sizable interannual variability (Hobbs et al., 2024), indicating

© 2024 The Author(s).

This is an open access article under the terms of the [Creative Commons Attribution-NonCommercial License](#), which permits use, distribution and reproduction in any medium, provided the original work is properly cited and is not used for commercial purposes.

that the Antarctic sea ice has shifted to a new state (Purich & Doddridge, 2023). In this context, the Antarctic sea ice prediction has increasingly gained interest for scientific purposes but also for practical demands due to increasing human activities (Grant et al., 2021; Rogers et al., 2020; Tejado et al., 2022).

Previous Antarctic sea ice prediction studies have mainly focused on seasonal scales. They have revealed several physical mechanisms affecting the Antarctic sea ice predictability, such as teleconnections originating from the tropical ocean (Liu et al., 2002; Wang, Luo, et al., 2023), the local ocean heat uptake and advection (Bushuk et al., 2021; Libera et al., 2022), stratospheric influences (Wang et al., 2021), and the sea ice thickness persistence (Morioka et al., 2021). Compared to the seasonal prediction, the subseasonal prediction (from two to 8 weeks), between seasonal and synoptic scales, has the best potential to support the planning of navigation routes (Dirkson et al., 2022; Wagner et al., 2020). Additionally, the processes on the subseasonal to seasonal timescales and the associated predictability mechanisms play a crucial role in constructing skillful seasonal predictions (Massonnet et al., 2023). However, the current knowledge of subseasonal predictability mechanisms is relatively scarce.

The Sea Ice Prediction Network South (SIPN South; Massonnet et al., 2018; Lieser et al., 2020) began in 2017, focusing mainly on the subseasonal to seasonal prediction of the summer Antarctic sea ice area. The SIPN forecast systems are classified as 'dynamical' or 'statistical'. The evaluation of SIPN South products showed that some statistical systems had a prediction skill equal to or better than dynamical systems (Massonnet et al., 2023). This suggests dynamical systems could be improved if they better capture the relevant dynamic and thermodynamic processes. However, Massonnet et al. (2023) evaluated summer months only, whereas a more comprehensive evaluation, including all months, is necessary to understand better the subseasonal prediction skill of dynamical systems.

Two subseasonal to seasonal Antarctic sea ice prediction data sets generated by dynamical systems are publicly available. The Subseasonal to Seasonal (S2S) Prediction Project (Vitart et al., 2017), implemented to facilitate a deeper understanding of S2S predictability and improve the S2S prediction skill, provides the first one. The evaluation of the S2S model forecasting skill suggests that the Antarctic sea ice prediction skill is, on average, 30% lower than in the Arctic, and only the European Center for Medium-Range Weather Forecasts (ECMWF) system forecasts are more skillful than climatological and persistence Antarctic sea ice forecasts (Zampieri et al., 2019). Since Zampieri et al. (2019), the S2S systems have been refined and updated, but it is unclear whether and to what extent their prediction skills have improved. The second data set is the Copernicus Climate Change Service (C3S) project (Thépaut et al., 2018) implemented by ECMWF, which includes daily Antarctic sea ice forecasts from eight prediction centers. Six centers were also involved in S2S but with different system configurations and smaller ensembles. The Antarctic sea ice prediction skill of C3S systems has not been assessed before.

This study is an extension of Zampieri et al. (2019) as it evaluates the latest S2S and C3S systems. Its objectives are twofold: first, to update the knowledge of dynamically modeled subseasonal Antarctic sea ice edge prediction skill and second, to identify factors that influence this prediction skill. It is essential to understand that its aim is not to oppose the S2S and C3S data sets, as they are not independent. However, it aims to support further development of dynamical Antarctic sea ice prediction systems analogously to what has already been carried out for Arctic systems (Bushuk et al., 2024).

2. Data and Methods

2.1. Data

The S2S and C3S sea ice reforecasts were evaluated over their common 14-year (2002–2015) period. Six C3S systems from six institutions were analyzed (Table 1). Although the C3S systems provided daily predictions for at least 6 months ahead, only the first 60 days were analyzed. The seven used S2S systems are listed in Table 2. Notably, the S2S systems were updated versions of those (ECMWF, UKMO, KMA, and MF) evaluated by Zampieri et al. (2019). Since the Hydrometeorological Center of Russia (HMCR) S2S system did not employ a dynamic sea ice model and resulted in significant errors (not shown), it was not included in the analysis.

The initial conditions (ICs) of each system are presented in Table 3. Notably, systems from a single institution participating in both projects are not entirely independent. Therefore, their intercomparison reveals the impacts of their different configurations. For example, the ECMWF system participating in both S2S and C3S share the

Table 1
List of C3S Systems Used in the Analysis and Their Configurations

| Institute ^a | System | Atmosphere ^b | Ocean | Sea ice | Ensemble size | Reforecast period | Forecast length |
|------------------------|---------------|---|---|--|------------------|-------------------|-----------------|
| CMCC | SPS3.5 | CESM 1.2-CAM 5.3 (~0.5°) | NEMO3.4 (0.25°) | CICE4.0 | 40 | 1993–2016 | 6 months |
| DWD | GCFS2.1 | ECHAM 6.3.05 (~100 km) | MPIOM 1.6.3 (0.4°) | Thermodynamic and sea-ice dynamics (included in MPIOM) | 30 | 1993–2019 | 6 months |
| ECCC | GEM5-NEMO | GEM (~110 km) | NEMO (1°; 1/3° meridionally near the equator) | CICE4.0 | 10 | 1990–2020 | 214 days |
| ECMWF | SEAS5 | IFS CY43R1 (~32 km) | NEMO3.4 (0.25°) | LIM2 | 25 | 1981–2016 | 215 days |
| MF ^c | System8 | ARPEGE v6.4 (~0.5°) | NEMO3.6 (0.25°) | GELATOv6 | 25 | 1993–2018 | 7 months |
| UKMO ^c | GloSea6-GC3.2 | Met Office Unified Model (UM) - Global Atmosphere 7.2 (0.83° × 0.56°) | NEMO3.6-Global Ocean 6.0 (0.25°) | CICE5.1.2-Global Sea-Ice 8.1 | 7 per start date | 1993–2016 | 215 days |

^aThe JMA system in the C3S project is not used since its coastal land mask covers too many areas with ice, seriously affecting the summer sea ice edge evaluation.

^bModel information was obtained from the C3S website. ^cAll the systems are initialized on the 1st of the month, except for MF (the MF ensembles are initialized using a lagged approach, but all the members are encoded as if they were initialized on the 1st of the month) and UKMO (the UKMO ensembles are initialized on 1st, 9th, 17th, 25th of the month).

ocean and sea ice models but not the ensemble size, so their intercomparison can, to some extent, reveal how the ensemble size influences their predictive performances.

The resolution of S2S and C3S data was 1° latitude × 1° longitude. The observational sea ice concentration reference product was based on the Global Sea Ice Concentration Climate Data Record, release 3 (OSI-450; OSI SAF, 2022) from the European Organization for the Exploitation of Meteorological Satellites (EUMETSAT) and was linearly interpolated onto the common. 1° latitude × 1° longitude grid for comparisons. Following Zampieri et al. (2019), a common conservative land mask was constructed by excluding the union of grid cells classified as land or missing values across all systems and observational products.

Table 2
As Table 1 but for S2S Systems

| Institute | System | Atmosphere ^a | Ocean | Sea ice | Ensemble size | Reforecast period | Forecast length |
|--------------------|--------------------|--|---------------------|------------------------------|---------------|-------------------|-----------------|
| ECCC | GEPS7 | GEM (~39 km) | NEMO3.6 (0.25°) | CICE4.0 | 4 | 2001–2020 | 32 days |
| ECMWF ^b | IFS | IFS CY47R3 (~16 km up to day 15 and ~32 km after day 15) | NEMO3.4.1 (0.25°) | LIM2 | 11 | Past 20 years | 46 days |
| IAP-CAS | CAS-FGOALS-f2-V1.3 | FAMIL (~100 km) | POP2 (1°) | CICE4 | 4 | 1999–2018 | 65 days |
| HMCRC | RUMS | SL-AV (Tolstykh et al., 2017) (0.9° × 0.72°) | N/A | N/A | 11 | 1991–2015 | 46 days |
| JMA | CPS3 | GSM2003C (Hirahara et al., 2023) (~55 km) | MRI.COMv4.6 (0.25°) | MOVE-G3 | 5 | 1991–2020 | 34 days |
| KMA ^b | GloSea6-GC3.2 | Met Office Unified Model Global Atmosphere (0.83° × 0.56°) | NEMO3.6 (0.25°) | CICE5.1.2 | 3 | 1993–2016 | 60 days |
| MF | CNRM-CM 6.1 | ARPEGEv6.3 (~50 km) | NEMO3.6 (0.25°) | GELATOv6 | 10 | 1993–2017 | 47 days |
| UKMO | HadGEM3-GC3.2 | Met Office Unified Model Global Atmosphere (0.83° × 0.56°) | NEMO3.6 (0.25°) | CICE5.1.2-Global Sea-Ice 8.1 | 7 | 1993–2016 | 60 days |

^aModel information for which references are not provided was obtained from the S2S website. ^bThe latest versions of the ECMWF and KMA systems are not used since their on-the-fly outputs could not cover a whole year. Therefore, the second-latest systems of these two are used.

Table 3
Information on the ICs Provided by the Nine Different Institutions

| Institute ^a | Atmospheric ICs | Oceanic ICs | Sec ice variables (data assimilation method) | References |
|------------------------|-----------------|---------------------|--|--|
| CMCC | ERA5 | C-GLORS | NSIDC SIC (Nudging) | Storto & Masina (2016); Gualdi et al. (2020) |
| DWD | ERA5 | ORAS5 | OSTIA SIC (Nudging) | Paxian et al. (2023); Zuo et al. (2019) |
| ECCC | ERA5 | ORAS5 | Interpolated monthly HadISST2.2 SIC and ORAS5 SIT (3D-Var) | Lin et al. (2020) |
| ECMWF | ERA-Interim | ORAS5 | OSTIA SIC (3D-Var) | Zuo et al. (2019) |
| MF | ERA5 | GLORYS12V1 | CERSAT SIC (Nudging) | Drévillon et al. (2023); Lellouche et al. (2021) |
| UKMO | ERA-Interim | GS-OSIA | OSI-SAF SIC (3D-Var) | MacLachlan et al. (2015) |
| JMA | JRA-3Q | MOVE/MRI.COM-G3 | A daily, quarter-degree operational SIC analysis (3D-Var) | Hirahara et al. (2023) |
| KMA | ERA-Interim | UKMO ODA reanalysis | OSI-SAF SIC (3D-Var) | Blockley et al. (2014); Kim et al. (2021) |
| IAP-CAS | JRA55 | GODAS | N/A ^b | Liu et al. (2023) |

^aFor a given institution, the sea ice ICs used by both the S2S and C3S systems are identical. ^bNo sea ice observations are directly assimilated and the sea ice initial conditions are determined by the atmospheric and oceanic conditions and their interactions with sea ice.

2.2. Sea Ice Edge Evaluation Metrics

Following Zampieri et al. (2019), we used the spatial probability score (SPS; Goessling & Jung, 2018) to quantify the prediction skill of the sea ice edge. SPS is the sum of overestimation (O) and underestimation (U):

$$O = \iint [\max(P_{\text{SIC}_f > 0.15}(x, y) - 1_{\text{SIC}_o > 0.15}(x, y), 0)]^2 dx dy, \quad (1)$$

$$U = \iint [\min(P_{\text{SIC}_f > 0.15}(x, y) - 1_{\text{SIC}_o > 0.15}(x, y), 0)]^2 dx dy, \quad (2)$$

where SIC is the sea ice concentration, the corner indices f and o indicate “forecast” and “observation”, respectively, $P_{\text{SIC}_f > 0.15}$ is the proportion of the ensemble members exceeding the 15% SIC threshold, which is also referred to as the modeled sea ice probability (SIP). The $1_{\text{SIC}_o > 0.15}$ maps elements of the $\text{SIC}_o > 0.15$ subset to one and all other elements to zero, also called the observational SIP. The 95% confidence intervals were computed based on the standard deviations obtained from all reforecasts. Additionally, since the SPS strongly correlates with the sea ice edge length (Palerm et al., 2019), the SPS was normalized for representative comparisons between the geographical sectors. The normalized SPS (Norm. SPS) was computed by dividing the SPS by the sea ice edge length following the approach by Melsom et al. (2019).

2.3. Benchmark Forecasts

The climatological prediction benchmark (CLIM-B) was calculated using the average of 10 years before the forecast. The damped anomaly persistence prediction benchmark (DAMP-B) was calculated following Yang et al. (2020):

$$S(t_0 + \delta t) = \text{CLIM}(t_0 + \delta t) + SA(t_0) \cdot r(t_0 + \delta t) \cdot \frac{\sigma(t_0 + \delta t)}{\sigma(t_0)}, \quad (3)$$

where S is the forecast variable, SA is its anomaly, r is the autocorrelation between the initial time and the target time, σ the standard deviation, t_0 the forecast initialization time, and $t_0 + \delta t$ is the forecast target time.

2.4. Multi-Model Forecasts

Building upon the systems above, we explore the potential advantages of multi-model ensemble predictions. Given that the S2S systems have different forecast initial times, we only constructed multi-model forecasts (MMFs) based on the C3S systems, whose predictions all started on the 1st day of the month (the UKMO forecasts started on the 1st, 9th, 17th, and 25th, but only forecasts starting on the 1st were used). Seven ensembles,

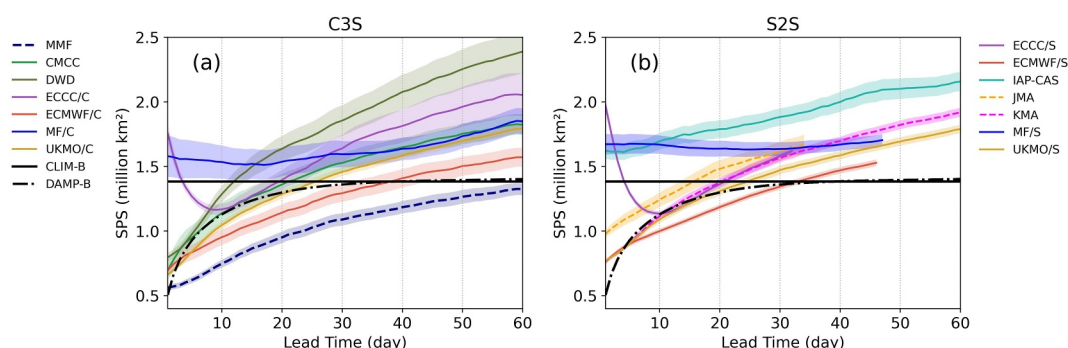


Figure 1. The SPS metrics of different systems in (a) the C3S project and (b) the S2S project. The SPS is averaged over the 14 years from 2002 to 2015 for all the initialization dates. Lower SPS values mean better sea ice edge prediction skill. Systems in both S2S and C3S projects are marked <system name+/S> and <system name+/C>, respectively. Different colors represent the systems of different institutions. The blue dashed line is the multi-model forecast (MMF). The shading indicates 95% confidence intervals, which are affected by the length of the time series.

equivalent to the smallest individual system ensemble size within the C3S system, were randomly selected from each system to form a 42-ensemble forecast. This approach ensured that the multi-model ensemble prediction skill was not skewed due to unequal individual system ensemble sizes.

3. Results

This section first presents the sea ice edge prediction skills of all C3S and S2S systems across the entire Southern Ocean. Then, seasonal and geographical sector results are shown regarding S2S variability (Zampieri et al., 2019) and the systems' ability to realistically consider the sources of predictability.

3.1. Overall Sea Ice Edge Prediction Skill

The SPSs varying with the leading day in both C3S and S2S projects' systems are shown in Figure 1. Systems that participated in both the S2S and C3S projects are marked <system name + /S> and <system name + /C>, respectively. Except for the MF and ECCC systems, SPS mean and spread increase with lead time. The ECMWF/C has about 38-day prediction skill compared to the CLIM-B, which is about five days longer than ECMWF/S. The UKMO systems are following, with their SPSs becoming worse than the CLIM-B after around 25 days. The ECCC systems initially have large errors, which decrease rapidly before 10 lead days and then maintain the predictive skill during the following 10 days. The MF SPSs are consistently above the CLIM-B but rarely increase with the lead time, indicating that the initial errors dominate the prediction performance. The comparison of the systems submitted to both S2S and C3S reveals that their prediction skills have benefited from the model updates. Compared to individual systems, the MMF has the best SPS-based prediction skill against benchmarks for up to 60 days.

The performance of three C3S systems (DWD, ECCC/C, and MF/C) and three S2S systems (IAP-CAS, JMA, and MF/S) consistently falls below that of DAMP-B. Among these, the JMA system demonstrates approximately 15 days of predictive skill relative to CLIM-B. The DWD SPS increases more rapidly than the other systems and becomes the least skillful C3S system after 8 days (except for MF/C). The IAP-CAS system performs worse than the CLIM-B, and its prediction skill declines steadily with lead time. In conclusion, systems exhibit various rates of error growth during the forecasting period, likely resulting from the differences in model initialization and configuration.

3.2. Regional Sea Ice Edge Prediction Skill

For the regional Norm. SPS-based system intercomparison, the Southern Ocean was divided into five geographical sectors (Bushuk et al., 2021). We found all C3S, S2S, and the CLIM-B benchmark have higher Norm. SPS values in the Weddell and Ross Seas than in the other sectors, while the western Pacific sector has relatively lower Norm. SPS values (Figures 2a–2l).

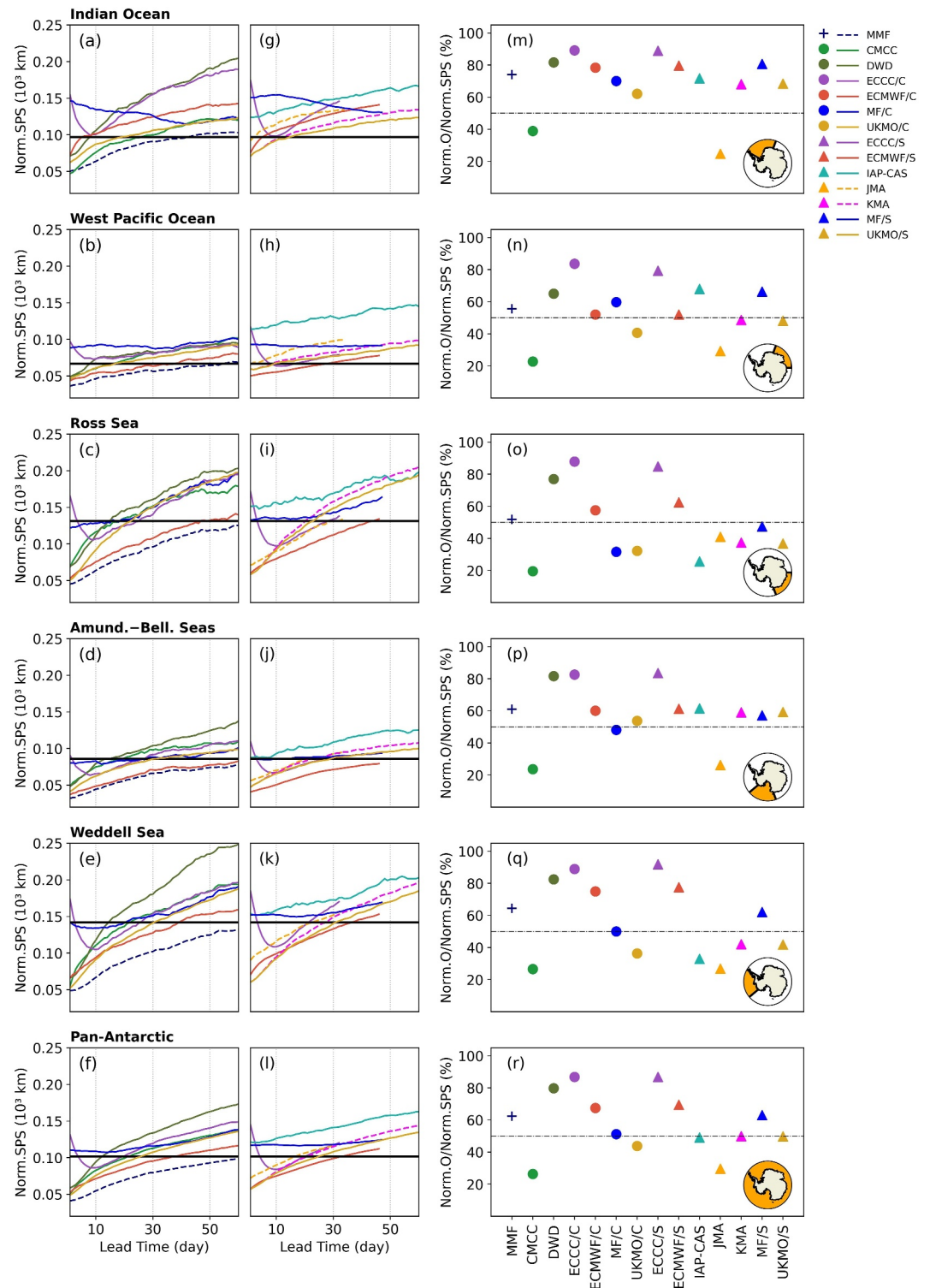


Figure 2. The Norm. SPS for each system in (a–f) the C3S project and (g–l) the S2S project in different geographical sectors. The black solid line in (a–l) is the CLIM-B. Panels (m–r) are the lead time averaged overestimation ratios; values higher than 50% indicate the overestimation of the sea ice edge dominates the Norm. SPS.

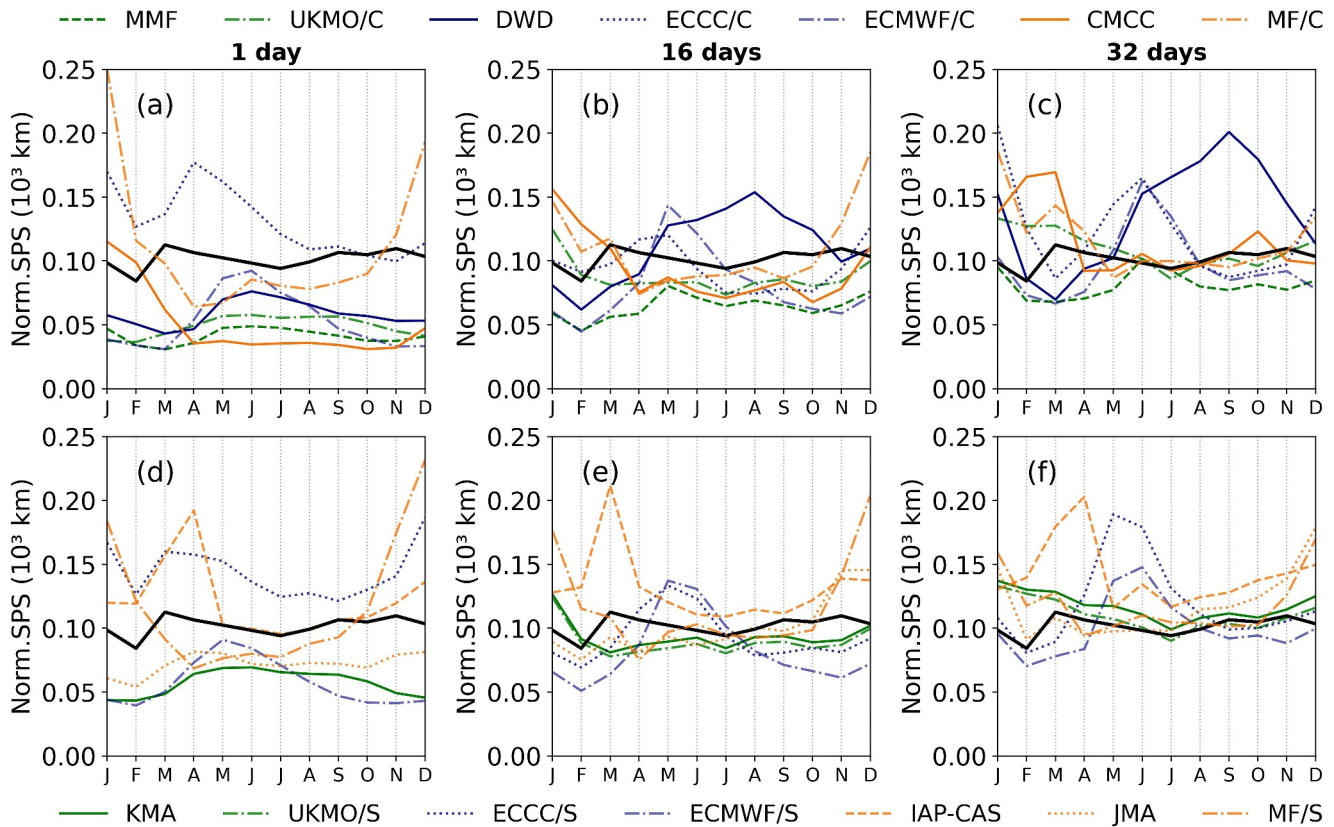


Figure 3. Monthly Norm. SPS metrics of (a–c) the C3S project and (d–f) the S2S project. The black solid line is the CLIM-B, and the columns indicate the 1st, 16th, and 32nd forecast days. The three groups (season independent, freezing bias, and melting bias) are depicted separately using three colors (green, dark blue, and light orange) separately. The curve representing KMA in (d) coincides precisely with UKMO/S.

Compared with the benchmarks, the dynamical systems demonstrate better skill in the western Antarctic sectors (i.e., the Weddell Sea, the Ross Sea, and the Amundsen and Bellingshausen Seas) than in the eastern sectors. For instance, the ECMWF/C has a 60-day prediction skill in the Amundsen and Bellingshausen Seas, a 50-day prediction skill in the Ross Sea but only a 5-day skill in the Indian Ocean sector. The MMF has consistently better skill than CLIM-B for 60 days except in the eastern Antarctic sectors. Despite some configuration changes from the S2S to the C3S, system regional prediction skill has remained mainly unchanged.

Figures 2m–2r illustrates that most systems simulated larger SIE than observed except in the Ross and Weddell Seas. The C3S and S2S DWD, ECCC, and ECMWF systems consistently overestimated the sea ice edge, whereas the CMCC and JMA systems underestimated the sea ice edge in all sectors. The MF, IAP-CAS, KMA, and UKMO systems both overestimated and underestimated the sea ice edge depending on the sector, resulting in, on average, good pan-Antarctic SIE. The MMF predictions present balanced predictions in the west Pacific and the Ross Sea but slightly overestimate the sea ice edge in other regions.

3.3. Seasonality of the Sea Ice Edge Prediction Skill

Figure 3 presents the monthly Norm. SPS for each system on the 1st, 16th, and 32nd lead days. Generally, the systems perform similarly (i.e., smaller spread of Norm. SPS) in winter but differently (i.e., more extensive spread of Norm. SPS) in summer. This seasonal difference in predictive skill can be used to classify systems into three groups. In the first group, the prediction skill is seasonally independent, including the MMF, KMA, and UKMO. In the second group, the prediction skill is worse in the freezing season (from April to September) than in the melting season (from October to March), including the DWD, ECCC, and ECMWF. Following Zampieri et al. (2019), these are so-called freezing-season bias systems. In the third group, the prediction skill is worse in the melting season than in the freezing season and labeled as the melting-transition bias systems (e.g., the CMCC, IAP-CAS, JMA, and MF). C3S and S2S systems from the same institute have similar Norm. SPS seasonal cycles.

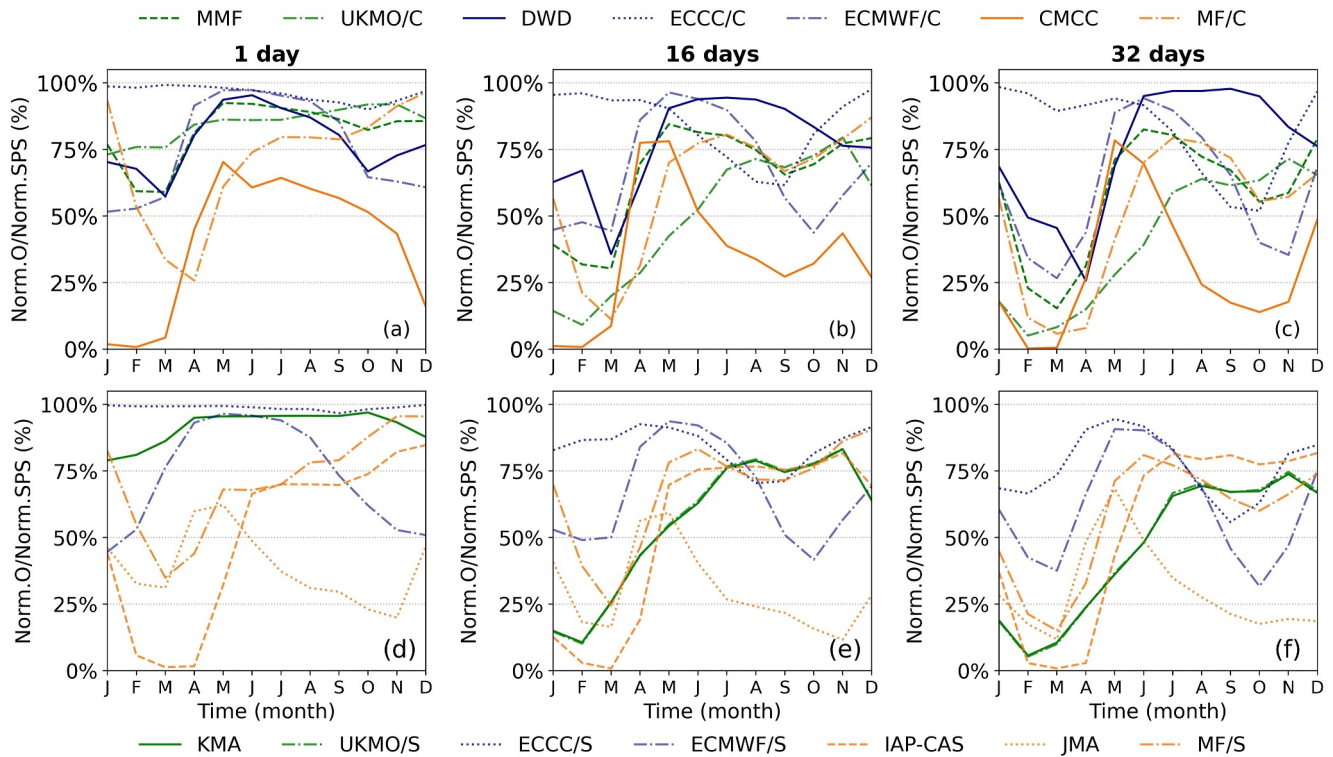


Figure 4. The overestimation proportion in different months of (a–c) the C3S project and (d–f) the S2S project. The columns indicate the 1st, 16th, and 32nd forecast days. The three groups (season independent, freezing bias, and melting bias) are depicted separately using three colors (green, dark blue, and light orange). The curve representing KMA in (d) coincides precisely with UKMO/S.

To analyze the identified SPS mismatches, the Norm. SPS was split into overestimated and underestimated components as shown by their ratios in Figure 4. The C3S and S2S systems (except UKMO and KMA) overestimate SIE during the freezing season and underestimate (or overestimate less) during the melting season. The proportion of the overestimation of the Norm. SPS decreases in summer and early spring (i.e., September to March next year) with the lead day.

By combining Figures 3 and 4, more detailed system seasonal performance can be diagnosed. Among the freezing-season bias systems, the DWD winter prediction skill declines as its lead time increases (Figures 3a–3c) partly due to the initial SIE overestimation (Figure 4a). On the other hand, the overestimation proportion increases with its lead time, implying that the DWD has a swift SIE growth rate. The ECMWF predictions perform better in other months than from May to July. This can be linked to its initial SIE overestimation during this period, persisting as the lead time increases (Figures 4a and 4d). The ECCC systems have significant initial SIE overestimations every month, which are exceptionally high in January and from March to June. However, the ECCC Norm. SPSs decrease from the 1st to about the 10th lead day (Figure 1). This may be caused by unrealistically low sea ice growth rates in the first few days of the forecast period or too early retreat in autumn (i.e., from April to June), resulting in an improved prediction skill during this period (Figure 3). Overall, initial SIE errors, comparably fast ice growth rates, and error propagation affect the performances of systems with the freezing season bias.

The performance of the systems with the melting-season bias is also linked to the initial SIE errors to a large extent. The CMCC system generally predicts the ice edge accurately except from December to March (Figure 3a), when its initial SIE is significantly underestimated at a level that persists as the model runs (Figures 4a–4c). This could be linked to the CMCC initial conditions from C-GLORS, which underestimates the Southern Ocean SIE especially in summer (Nie et al., 2022; Uotila et al., 2019). Also, the IAP-CAS prediction skill declines due to the initial underestimations but only from March to May. The MF forecast system skill is inferior to CLIM-B (Figure 1) primarily due to significant initial errors in spring and summer (Figures 3a and 3d) characterized by the overestimated Norm. SPSs (Figures 4a and 4d). Although the JMA initial error is small, its SPS significantly

increases when its lead time extends in the melting season (i.e., from October to January) in contrast with its performance in other seasons.

In summary, the seasonal initial error can determine the bias type well. The initial error propagation also depends on the model's physics, affecting the bias evolution.

4. Discussion

4.1. Relative Roles of Initialization and Model Physics

As discussed in the previous sections, initialization is essential when predicting at a subseasonal timescale. However, several systems did not initialize sea ice properly. For example, the ECCO systems initially overestimated SIE (Figures 3 and 4). This could have been related to their initialization routine, where monthly HadISST2.2 SIC data were interpolated to daily values (Table 3). The IAP-CAS did not assimilate sea ice observations to improve the initialization, resulting in a large SPS (Figure 1b) maintained until day 32 (Figures 3 and 4). In contrast, CERSAT constantly underestimated SIE relative to the OSI-450 (Lellouche et al., 2021); hence, the initial anomalous SPS overestimation by the MF during the sea ice melt season cannot be easily explained by the assimilated SIC data.

The other C3S and S2S systems initialized sea ice more realistically. The CMCC, UKMO/C, and ECMWF/C systems from the C3S project had comparable SPSs on day 1 but were more prominent than the DAMP-B benchmark. However, CMCC and UKMO/C SPSs increased more rapidly than ECMWF/C during the first 10 days. Similarly, the S2S KMA, UKMO/S, and ECMWF/S systems had nearly identical initial SPSs, but the first two increased faster than ECMWF/S during the first 10 days. These differences in SPS rates suggest that the initialization error propagation is system dependent.

We computed the SIP (the ensemble-based probability of SIC being above 15%; see Section 2.2 for details) biases for the dynamical system predictions to verify this conclusion (Figure 5). The C3S CMCC and the S2S JMA systems underestimated SIP slightly on the first day but very clearly on the 32nd day. In contrast, those systems that overestimated SIP on the first day demonstrated two error propagation types: (a) in DWD and ECMWF systems the SIP overestimation increased; (b) in UKMO and KMA systems the SIP overestimation decreased and became underestimation on day 32, particularly in the inner pack ice regions, implying a complex error propagation with the forecast time.

In summary, although reasonable initial conditions are necessary for a system to have subseasonal predictive capability, they are insufficient. The system-dependent propagation of initial errors suggests that the model physics is crucial in determining the system's predictive capability and should be given equal attention as system initialization. Furthermore, experiments conducted over longer-than-subseasonal timescales indicate that the initialization dominance varies seasonally (Goosse et al., 2023). During the early sea ice growth season, sea ice predictions primarily rely on the gradually diminishing solar radiation. For example, as discussed in Section 3.3, those systems with the freezing season bias are significantly influenced by initialization errors early in the freezing season. In contrast, the increasing solar radiation complicates the prediction of sea ice evolution during the melting season. At this point, initialization and model physics influence sea ice prediction, causing errors to propagate in complex ways and not just simply to increase with lead time, as was the case of UKMO and KMA systems. These two systems had negative summer biases in the inner pack ice reversed from the winter positive biases at the beginning (Figure 5). In summary, the system classification presented in Section 3.3 can alternatively be understood as an error source classification.

4.2. Impact of Ensemble Size on the SPS Metric

In addition to the more realistic MMF initial state than those of individual systems (Figure 1), its remarkable performance in terms of SPS probably also results from its larger ensemble size and the cancellation of individual system biases. These findings are consistent with the Arctic sea ice predictions analyzed by Bushuk et al. (2024). To analyze the SPS dependence on the system ensemble size, we randomly downsampled the ensemble sizes of individual C3S systems with more than 10 ensemble members and the MMF system. By repeating the sampling 10 times, new 10-member CMCC, DWD, ECMWF, and MF ensembles were generated. Furthermore, ten 6-member C3S MMF ensembles were generated by randomly selecting one member from each C3S individual system ensemble.

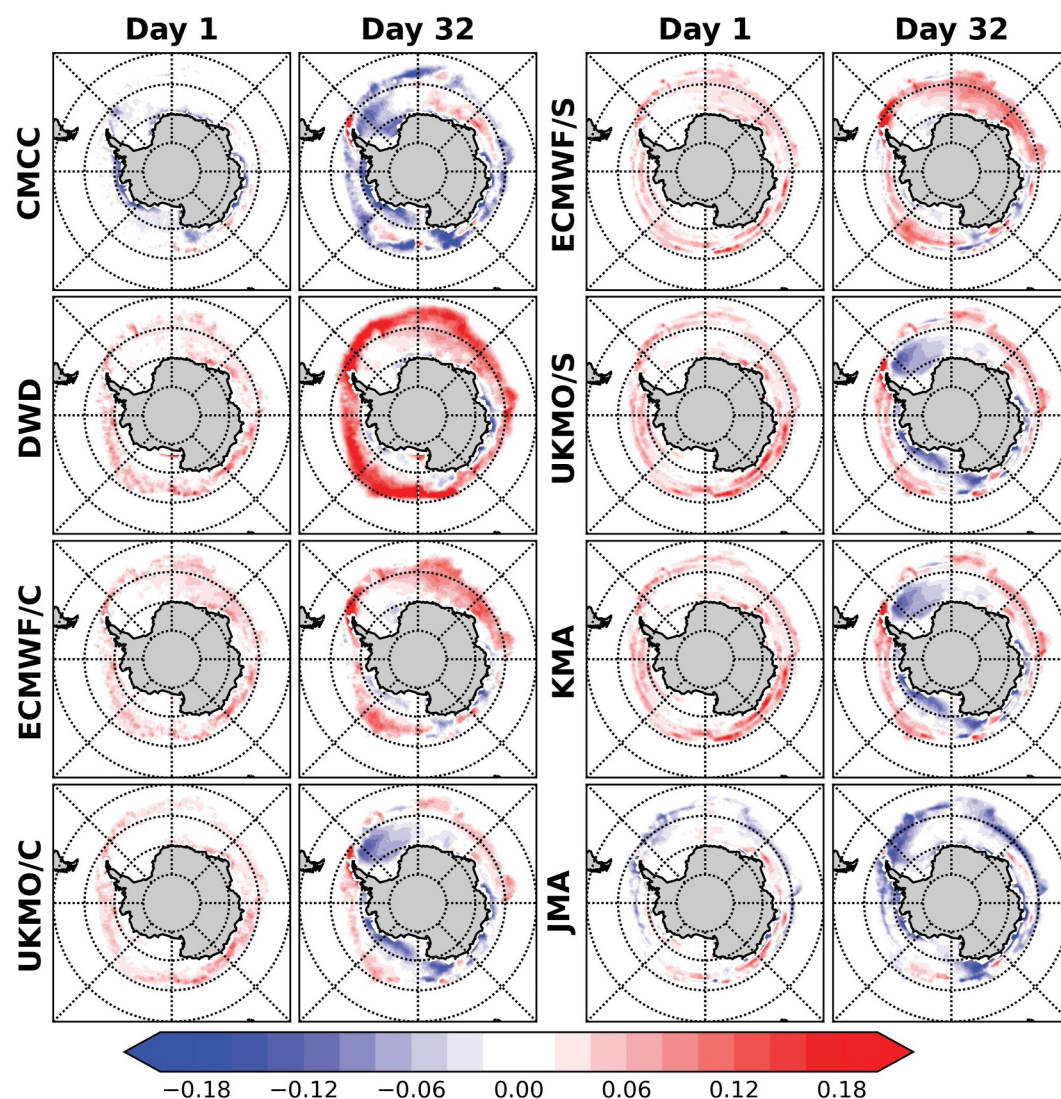


Figure 5. The 14-year averaged (2002–2015) spatial distribution of SIP biases (“model” minus “observation”) for different systems on the 1st and the 32nd lead day.

The 6-member MMF forecasts consistently outperform the 10-member forecasts (Figure 6) and surpass the individual C3S system forecasts before downsampling. This demonstrates that the good MMF performance (Figure 1) is not solely attributable to its larger ensemble size compared to the individual systems but also benefits from its ability to cancel out individual system biases. The ensemble size is an essential factor influencing the system performance on the SPS metric also in the Arctic (Goessling & Jung, 2018). Sampling down the ensemble size always reduces the prediction skill that amplifies with the lead time (Figure 6). The behavior of similarly configured KMA and UKMO/S systems highlights this. These two systems have identical atmospheric, oceanic, and sea ice modules, and the initialization (except the initial ocean conditions). Due to this, their regional and seasonal prediction characteristics look similar (Figures 2 and 3). However, their ensemble sizes differ (UKMO/S has 7 members, whereas KMA has 3), so that after 10 days, the KMA SPS starts to increase faster than the UKMO/S SPS and has approximately 5 days shorter predictive skill than the UKMO/S (Figure 1).

To conclude, the good MMF predictive skill compared to individual systems is primarily due to the inter-system bias cancellations. In addition, increasing the ensemble size further improves the predictive skill under the SPS metric in the MMF and individual systems.

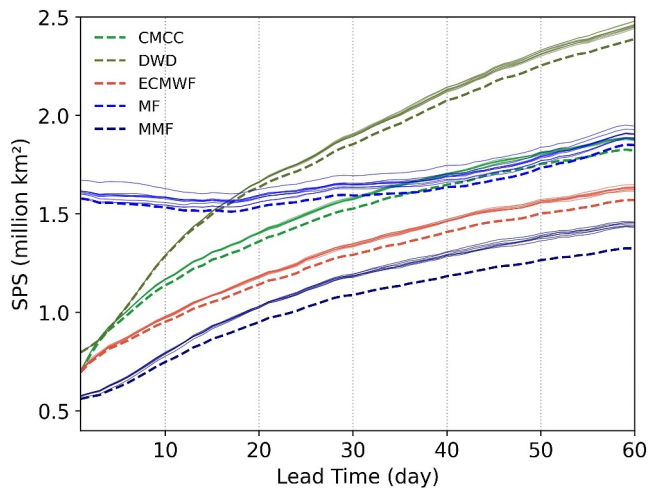


Figure 6. The SPS of the C3S systems and MMF with downsampling ensemble size. The systems with more than 10 ensemble sizes are tested, and 10 ensembles are randomly selected from all the ensembles 10 times. The downsampling MMF includes six ensembles, and the ensembles are from different systems. The thinner solid lines are the downsampling results, and the thicker dashed lines are the original SPSs shown in Figure 1a.

4.3. Evaluation With Deterministic Metric

A deterministic comparison was carried out besides the probabilistic evaluation. To quantify the prediction error, the integrated ice-edge error (IIEE; Goessling et al., 2016) metric, which estimates the mismatch between the ensemble mean predicted sea ice edge and observations (e.g., Dong et al., 2024; Lin et al., 2021; Wang, Luo, et al., 2023), was calculated.

Despite the similarities between the IIEE-based results (Figures 7a and 7b) and the SPS-based results (Figure 1), there are some deviations. For example, the IIEE predictive skill was better than the SPS predictive skill against the CLIM-B benchmark. The UKMO SPS measured skill lasted up to 47 days, surpassing the ECMWF/C (~42 days) as the best-performing dynamical prediction system. In addition, the best UKMO ensemble member had a prediction skill of 38 days, 9 days less than the ensemble mean (Figures 7a and 7c). The ECMWF/C ensemble member predictive skill was only 30 days also significantly less than the ensemble mean of ~40 days. Surprisingly, the IIEE-measured MMF predictive skill was about as good as the UKMO. This may be due to the well-dispersed multi-model ensembles related to uneven prediction skill distribution (Weigel et al., 2008). As a supplement to Section 4.2, this characteristic, on the other hand, enhances the prediction skill score under the SPS probabilistic metric.

Based on these results, we argue that no individual member of the ECMWF ensemble performs well when measured with the IIEE metric, which contrasts

the UKMO C3S or S2S ensembles. This finding is significant when applying deep learning methods to evaluate Antarctic sea ice predictions. Our results suggest that particular care is needed when validating subseasonal sea ice predictions because probabilistic and deterministic metrics must be balanced.

5. Conclusions

Using the SPS probabilistic metric, we evaluated the Antarctic sea ice edge prediction skill of the C3S and S2S dynamical systems. Our results indicate that individual dynamic systems skillfully predict the ice edge up to 38 days in advance. Compared to separate systems and observational benchmarks, the C3S multi-model forecast MMF had the best predictive capability. The dynamic system predictive skill varies significantly across different Antarctic geographic sectors, generally showing more accurate forecasts in the western Antarctic than in the eastern Antarctic, where SIE is often overestimated. The predictive skill per season was primarily system

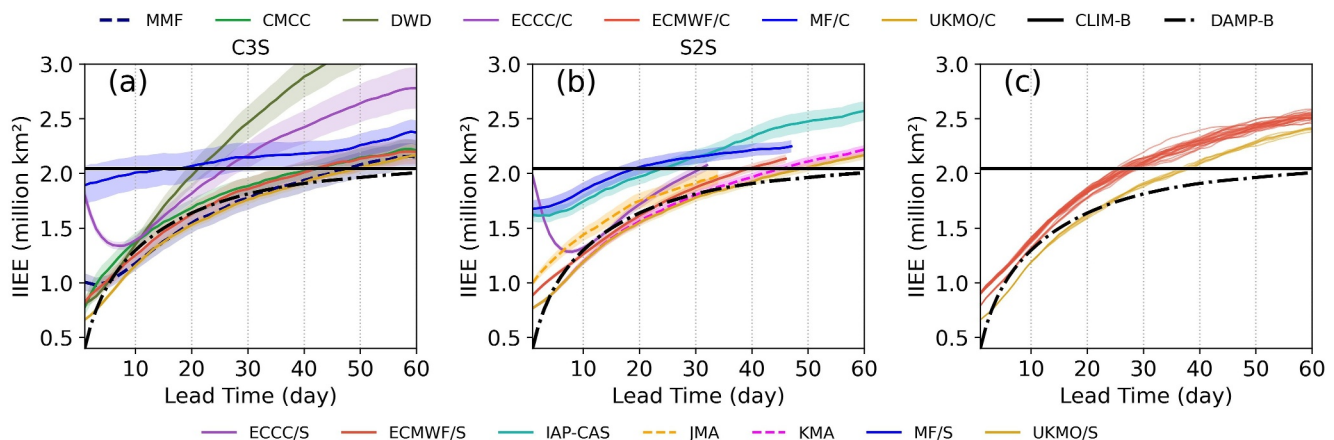


Figure 7. As Figure 1, but for IIEE metric for (a) the C3S systems and (b) the S2S systems. The single ensemble IIEEs of the ECMWF/C and the UKMO/C are presented in (c).

dependent, as some systems had a freezing-season bias, some had a melting-season bias, and some had biases without seasonal dependence.

Our analysis of the system prediction skill highlights the importance of initial conditions, as those systems initialized with the most unrealistic SIE did not skillfully predict the sea ice edge. This could be why observational data-driven sea ice prediction systems generally have better predictive skills than dynamical systems (Dong et al., 2024; Massonnet et al., 2023). In the coming years, the assessments of subseasonal and seasonal forecast skills by systems using machine learning-based data assimilation techniques (e.g., the work of Geer, 2023, on the operational ECMWF prediction system) should be given priority.

For the systems with similar initial sea ice states, individual error propagation indicates that the model physics significantly impacts their prediction. Reducing sea ice biases requires improving its dynamics, thermodynamics, and external drivers (Nie et al., 2023). Moreover, understanding these mechanisms will also benefit the development of the emerging deep learning-based Antarctic sea ice prediction (Eayrs et al., 2024). This study showed that the straightforwardly and operationally applicable MMF had a smaller bias than individual systems. This has been a helpful approach in the Arctic sea ice prediction (Batté et al., 2020; Harnos et al., 2019) and in the Antarctic summer sea ice prediction (Massonnet et al., 2023, Table 2). In addition to the initialization and model physics, the ensemble size and spread (Goessling & Jung, 2018) impacted the sea ice predictive skill.

Dynamical system prediction skills differed depending on the evaluation metrics. The ECMWF/C had the best predictive skill when using SPS, whereas the UKMO systems had the best skill according to IIEE. This discrepancy was related to their ensemble distributions and the SPS and IIEE properties. Although our conclusions are based on reforecasts, they could be extended to operational forecasts with the same initialization routines and models (Goddard et al., 2012). For instance, the systems with the freezing-season bias (e.g., the ECMWF) cannot comparably provide skillful sea ice edge predictions for the 2023 and 2024 freezing seasons (not shown) when the ice growth rates were meager. Finally, this study does not address how the complex Antarctic air-ice-ocean interactions (Goosse et al., 2023; Himmich et al., 2023) and the external drivers will impact the dynamic system subseasonal prediction skill. In the future, a comprehensive analysis of modeled sea ice velocity, thickness, and oceanic variables (e.g., sea surface currents, temperature, and oceanic heat transport) could be conducted due to their better availability (e.g., Xiu et al., 2022).

Data Availability Statement

All data analyses here are open-accessible. The OSI-450-a SIC data used for analysis in this study can be downloaded from OSI SAF (2022). The model data from the C3S and S2S projects are available at <https://cds.climate.copernicus.eu/datasets/seasonal-original-single-levels?tab=download> and <https://apps.ecmwf.int/datasets/data/s2s-reforecasts-instantaneous-accum-ecmf/levtype=sfc/type=cf/>, respectively.

Acknowledgments

This study was supported by the National Key Research and Development Program of China (2022YFE0106300), the Southern Marine Science and Engineering Guangdong Laboratory (Zhuhai) (SML2021SP201, SML2022SP401, SML2023SP207, and SML2023SP219), the China Postdoctoral Science Foundation (Grant 2023M741526), and the Norges Forskningsråd (328886). Petteri Uotila was supported by the Academy of Finland (project 355783) and the European Union's Horizon 2020 research and innovation framework program (PolarRES project, Grant 101003590). Lorenzo Zampieri was supported by the European Union's Horizon 2020 research and innovation program under Grant agreement No. 101003826 via the project CRiceS (Climate Relevant interactions and feedback: the key role of sea ice and snow in the polar and global climate system).

References

- Bader, J., Flügge, M., Kvamstø, N. G., Mesquita, M. D. S., & Voigt, A. (2013). Atmospheric winter response to a projected future Antarctic sea-ice reduction: A dynamical analysis. *Climate Dynamics*, 40(11–12), 2707–2718. <https://doi.org/10.1007/s00382-012-1507-9>
- Batté, L., Välisuo, I., Chevallier, M., Acosta Navarro, J. C., Ortega, P., & Smith, D. (2020). Summer predictions of Arctic sea ice edge in multi-model seasonal re-forecasts. *Climate Dynamics*, 54(11–12), 5013–5029. <https://doi.org/10.1007/s00382-020-05273-8>
- Blockley, E. W., Martin, M. J., McLaren, A. J., Ryan, A. G., Waters, J., Lea, D. J., et al. (2014). Recent development of the met office operational ocean forecasting system: An overview and evaluation of the new global FOAM forecasts. *Geoscientific Model Development*, 7(6), 2613–2638. <https://doi.org/10.5194/gmd-7-2613-2014>
- Bushuk, M., Ali, S., Bailey, D. A., Bao, Q., Batté, L., Bhatt, U. S., et al. (2024). Predicting September Arctic Sea Ice: A multi-model seasonal skill comparison. *Bulletin of the American Meteorological Society*, 105(7), E1170–E1203. <https://doi.org/10.1175/BAMS-D-23-0163.1>
- Bushuk, M., Winton, M., Haumann, F. A., Delworth, T., Lu, F., Zhang, Y., et al. (2021). Seasonal prediction and predictability of regional Antarctic sea ice. *Journal of Climate*, 34(15), 1–68. <https://doi.org/10.1175/JCLI-D-20-0965.1>
- Dirkson, A., Denis, B., Merryfield, W. J., Peterson, K. A., & Tietsche, S. (2022). Calibration of subseasonal sea-ice forecasts using ensemble model output statistics and observational uncertainty. *Quarterly Journal of the Royal Meteorological Society*, 148(747), 2717–2741. <https://doi.org/10.1002/qj.4332>
- Dong, X., Yang, Q., Nie, Y., Zampieri, L., Wang, J., Liu, J., & Chen, D. (2024). Antarctic sea ice prediction with A convolutional long short-term memory network. *Ocean Modelling*, 190, 102386. <https://doi.org/10.1016/j.ocemod.2024.102386>
- Drévillon, M., Fernandez, E., & Lellouche, J. M. (2023). GLOBAL_MULTIYEAR_PHY_001_030, (1).
- Eayrs, C., Lee, W. S., Jin, E., Lemieux, J.-F., Massonnet, F., Vancoppenolle, M., et al. (2024). Advances in machine learning techniques can assist across a variety of stages in Sea Ice applications. *Bulletin of the American Meteorological Society*, 105(3), E527–E531. <https://doi.org/10.1175/BAMS-D-23-0332.1>
- Geer, A. (2023). Combining machine learning and data assimilation to estimate sea ice concentration. <https://doi.org/10.21957/AGH93VS26>

- Goddard, L., Kumar, A., Solomon, A., Smith, D., Boer, G., Gonzalez, P., et al. (2013). A verification framework for interannual-to-decadal predictions experiments. *Climate Dynamics*, 40(1–2), 245–272. <https://doi.org/10.1007/s00382-012-1481-2>
- Goessling, H. F., & Jung, T. (2018). A probabilistic verification score for contours: Methodology and application to Arctic ice-edge forecasts. *Quarterly Journal of the Royal Meteorological Society*, 144(712), 735–743. <https://doi.org/10.1002/qj.3242>
- Goessling, H. F., Tietsche, S., Day, J. J., Hawkins, E., & Jung, T. (2016). Predictability of the Arctic sea ice edge. *Geophysical Research Letters*, 43(4), 1642–1650. <https://doi.org/10.1002/2015GL067232>
- Goosse, H., Allende Contador, S., Bitz, C. M., Blanchard-Grigglesworth, E., Eayrs, C., Fichefet, T., et al. (2023). Modulation of the seasonal cycle of the Antarctic sea ice extent by sea ice processes and feedbacks with the ocean and the atmosphere. *The Cryosphere*, 17(1), 407–425. <https://doi.org/10.5194/tc-17-407-2023>
- Grant, S. M., Waller, C. L., Morley, S. A., Barnes, D. K. A., Brasier, M. J., Double, M. C., et al. (2021). Local drivers of change in Southern Ocean ecosystems: Human activities and policy implications. *Frontiers in Ecology and Evolution*, 9, 624518. <https://doi.org/10.3389/fevo.2021.624518>
- Gualdi, S., Borrelli, A., Cantelli, A., Davoli, G., Del Mar Chaves Montero, M., Masina, S., et al. (2020). The new CMCC operational seasonal prediction system SPS3.5. *CM*. <https://doi.org/10.25424/CMCC/SPS3.5>
- Harnos, K. J., L'Heureux, M., Ding, Q., & Zhang, Q. (2019). Skill of seasonal arctic Sea Ice extent predictions using the North American multi-model ensemble. *Journal of Climate*, 32(2), 623–638. <https://doi.org/10.1175/JCLI-D-17-0766.1>
- Haumann, F. A., Gruber, N., Münnich, M., Frenger, I., & Kern, S. (2016). Sea-ice transport driving Southern Ocean salinity and its recent trends. *Nature*, 537(7618), 89–92. <https://doi.org/10.1038/nature19101>
- Himmich, K., Vancoppenolle, M., Madec, G., Sallée, J.-B., Holland, P. R., & Lebrun, M. (2023). Drivers of Antarctic sea ice advance. *Nature Communications*, 14(1), 6219. <https://doi.org/10.1038/s41467-023-41962-8>
- Hirahara, S., Kubo, Y., Yoshida, T., Komori, T., Chiba, J., Takakura, T., et al. (2023). Japan meteorological agency/meteorological research institute coupled prediction system version 3 (JMA/MRI-CPS3). *Journal of the Meteorological Society of Japan. Ser. II*, 101(2), 149–169. <https://doi.org/10.2151/jmsj.2023-009>
- Hobbs, W., Spence, P., Meyer, A., Schroeter, S., Fraser, A. D., Reid, P., et al. (2024). Observational evidence for a regime shift in summer Antarctic Sea Ice. *Journal of Climate*, 37(7), 2263–2275. <https://doi.org/10.1175/JCLI-D-23-0479.1>
- Jenouvrier, S., Holland, M., Stroeve, J., Serreze, M., Barbraud, C., Weimerskirch, H., & Caswell, H. (2014). Projected continent-wide declines of the emperor penguin under climate change. *Nature Climate Change*, 4(8), 715–718. <https://doi.org/10.1038/nclimate2280>
- Kim, H., Lee, J., Hyun, Y.-K., & Hwang, S.-O. (2021). The KMA global seasonal forecasting system (GloSea6) - Part 1: Operational system and improvements. *Atmosphere*, 31(3), 341–359. <https://doi.org/10.14191/ATMOS.2021.31.3.341>
- Lellouche, J.-M., Eric, G., Romain, B.-B., Gilles, G., Angélique, M., Marie, D., et al. (2021). The Copernicus global 1/12° oceanic and Sea Ice GLORYS12 reanalysis. *Frontiers in Earth Science*, 9, 698876. <https://doi.org/10.3389/feart.2021.698876>
- Libera, S., Hobbs, W., Klocker, A., Meyer, A., & Matear, R. (2022). Ocean-Sea Ice processes and their role in multi-month predictability of Antarctic Sea Ice. *Geophysical Research Letters*, 49(8). <https://doi.org/10.1029/2021GL097047>
- Lieser, J. L., Massonnet, F., Hobbs, W., Fyfe, J., Bitz, C. M., & Reid, P. (2020). Sea ice prediction network-south: Coordinating Seasonal predictions of Sea ice for the Southern Ocean. *Bulletin of the American Meteorological Society*, 101(8), S313–S315. <https://doi.org/10.1175/BAMS-D-20-0090.1>
- Lin, H., Merryfield, W. J., Muncaster, R., Smith, G. C., Markovic, M., Dupont, F., et al. (2020). The Canadian seasonal to interannual prediction system version 2 (CanSIPSv2). *Weather and Forecasting*, 35(4), 1317–1343. <https://doi.org/10.1175/WAF-D-19-0259.1>
- Lin, X., Massonnet, F., Fichefet, T., & Vancoppenolle, M. (2021). SITool (v1.0) – A new evaluation tool for large-scale sea ice simulations: Application to CMIP6 OMIP. *Geoscientific Model Development*, 14(10), 6331–6354. <https://doi.org/10.5194/gmd-14-6331-2021>
- Liu, A., Yang, J., Bao, Q., He, B., Wu, X., Liu, J., et al. (2023). Subseasonal-to-seasonal prediction of arctic sea ice Using a Fully Coupled dynamical ensemble forecast system. *Atmospheric Research*, 295, 107014. <https://doi.org/10.1016/j.atmosres.2023.107014>
- Liu, J., Yuan, X., Rind, D., & Martinson, D. G. (2002). Mechanism study of the ENSO and southern high latitude climate teleconnections. *Geophysical Research Letters*, 29(14). <https://doi.org/10.1029/2002GL015143>
- MacLachlan, C., Arribas, A., Peterson, K. A., Maidens, A., Fereday, D., Scaife, A. A., et al. (2015). Global seasonal forecast system version 5 (GloSea5): A high-resolution seasonal forecast system. *Quarterly Journal of the Royal Meteorological Society*, 141(689), 1072–1084. <https://doi.org/10.1002/qj.2396>
- Massonnet, F., Barreira, S., Barthélemy, A., Bilbao, R., Blanchard-Grigglesworth, E., Blockley, E., et al. (2023). SIPN South: Six years of coordinated seasonal Antarctic sea ice predictions. *Frontiers in Marine Science*, 10, 1148899. <https://doi.org/10.3389/fmars.2023.1148899>
- Massonnet, F., Reid, P., Lieser, J. L., Bitz, C. M., Fyfe, J., Hobbs, W., & Kusahara, K. (2018). Evaluation of February 2018 sea-ice forecasts for the Southern Ocean (No. UCL-Université Catholique de Louvain). *Technical report, Antarctic Climate & Ecosystems Cooperative Research Centre, Hobart, Tasmania*, 2018. <https://eprints.utas.edu.au/27184>
- Melsom, A., Palermé, C., & Müller, M. (2019). Validation metrics for ice edge position forecasts. *Ocean Science*, 15(3), 615–630. <https://doi.org/10.5194/os-15-615-2019>
- Morioka, Y., Iovino, D., Cipollone, A., Masina, S., & Behera, S. K. (2021). Summertime sea-ice prediction in the Weddell Sea improved by sea-ice thickness initialization. *Scientific Reports*, 11(1), 11475. <https://doi.org/10.1038/s41598-021-91042-4>
- Nie, Y., Lin, X., Yang, Q., Liu, J., Chen, D., & Uotila, P. (2023). Differences between the CMIP5 and CMIP6 Antarctic Sea Ice concentration budgets. *Geophysical Research Letters*, 50(23), e2023GL105265. <https://doi.org/10.1029/2023GL105265>
- Nie, Y., Uotila, P., Cheng, B., Massonnet, F., Kimura, N., Cipollone, A., & Lv, X. (2022). Southern Ocean sea ice concentration budgets of five ocean-sea ice reanalyses. *Climate Dynamics*, 59(11–12), 3265–3285. <https://doi.org/10.1007/s00382-022-06260-x>
- OSI SAF (2022). Global sea ice concentration climate data record 1978–2020 (v3.0), OSI-450-a. https://doi.org/10.15770/EUM_SAF_OSI_0013. *EUROPEAN SPACE AGENCY*. accessed 26-09-2023.
- Palermé, C., Müller, M., & Melsom, A. (2019). An intercomparison of verification scores for evaluating the Sea Ice edge position in seasonal forecasts. *Geophysical Research Letters*, 46(9), 4757–4763. <https://doi.org/10.1029/2019GL082482>
- Paxian, A., Mannig, B., Tivig, M., Reinhardt, K., Isensee, K., Pasternack, A., et al. (2023). The DWD climate predictions website: Towards a seamless outlook based on subseasonal, seasonal and decadal predictions. *Climate Services*, 30, 100379. <https://doi.org/10.1016/j.cliser.2023.100379>
- Purich, A., & Doddridge, E. W. (2023). Record low Antarctic sea ice coverage indicates a new sea ice state. *Communications Earth & Environment*, 4(1), 314. <https://doi.org/10.1038/s43247-023-00961-9>
- Rogers, A. D., Frinault, B. A. V., Barnes, D. K. A., Bindoff, N. L., Downie, R., Ducklow, H. W., et al. (2020). Antarctic futures: An evaluation of climate-driven changes in ecosystem structure, function, and service provisioning in the Southern Ocean. *Annual Review of Marine Science*, 12(1), 87–120. <https://doi.org/10.1146/annurev-marine-010419-011028>

- Storto, A., Masina, S., & Navarra, A. (2016). Evaluation of the CMCC eddy-permitting global ocean physical reanalysis system (C-GLORS, 1982–2012) and its assimilation components. *Quarterly Journal of the Royal Meteorological Society*, 142(695), 738–758. <https://doi.org/10.1002/qj.2673>
- Tejedo, P., Benayas, J., Cajiao, D., Leung, Y.-F., De Filippo, D., & Liggett, D. (2022). What are the real environmental impacts of Antarctic tourism? Unveiling their importance through a comprehensive meta-analysis. *Journal of Environmental Management*, 308, 114634. <https://doi.org/10.1016/j.jenvman.2022.114634>
- Thépaut, J.-N., Dee, D., Engelen, R., & Pinty, B. (2018). The Copernicus programme and its climate change service. In *Igarss 2018 - 2018 IEEE international geoscience and remote sensing symposium* (pp. 1591–1593). IEEE. <https://doi.org/10.1109/IGARSS.2018.8518067>
- Tolstykh, M., Shashkin, V., Fadeev, R., & Goyman, G. (2017). Vorticity-divergence semi-Lagrangian global atmospheric model SL-AV20: Dynamical core. *Geoscientific Model Development*, 10(5), 1961–1983. <https://doi.org/10.5194/gmd-10-1961-2017>
- Uotila, P., Goosse, H., Haines, K., Chevallier, M., Barthélemy, A., Bricaud, C., et al. (2019). An evaluation of ten ocean reanalyses in the polar regions. *Climate Dynamics*, 52(3–4), 1613–1650. <https://doi.org/10.1007/s00382-018-4242-z>
- Vitart, F., Ardilouze, C., Bonet, A., Brookshaw, A., Chen, M., Codorean, C., et al. (2017). The subseasonal to seasonal (S2S) prediction project database. *Bulletin of the American Meteorological Society*, 98(1), 163–173. <https://doi.org/10.1175/BAMS-D-16-0017.1>
- Wagner, P. M., Hughes, N., Bourbonnais, P., Stroeve, J., Rabenstein, L., Bhatt, U., et al. (2020). Sea-ice information and forecast needs for industry maritime stakeholders. *Polar Geography*, 43(2–3), 160–187. <https://doi.org/10.1080/1088937X.2020.1766592>
- Wang, J., Luo, H., Yu, L., Li, X., Holland, P. R., & Yang, Q. (2023). The impacts of combined SAM and ENSO on seasonal Antarctic Sea Ice changes. *Journal of Climate*, 36(11), 3553–3569. <https://doi.org/10.1175/JCLI-D-22-0679.1>
- Wang, S., Liu, J., Cheng, X., Kerzenmacher, T., Hu, Y., Hui, F., & Braesicke, P. (2021). How do weakening of the stratospheric polar vortex in the southern hemisphere affect regional Antarctic Sea Ice extent? *Geophysical Research Letters*, 48(11), e2021GL092582. <https://doi.org/10.1029/2021GL092582>
- Wang, Y., Yuan, X., Ren, Y., Bushuk, M., Shu, Q., Li, C., & Li, X. (2023). Subseasonal prediction of regional Antarctic Sea Ice by a deep learning model. *Geophysical Research Letters*, 50(17), e2023GL104347. <https://doi.org/10.1029/2023GL104347>
- Xiu, Y., Luo, H., Yang, Q., Tietsche, S., Day, J., & Chen, D. (2022). The challenge of arctic Sea Ice thickness prediction by ECMWF on subseasonal time scales. *Geophysical Research Letters*, 49(8). <https://doi.org/10.1029/2021GL097476>
- Yang, C., Liu, J., & Xu, S. (2020). Seasonal arctic Sea Ice prediction using a newly developed fully coupled regional model with the assimilation of satellite Sea Ice observations. *Journal of Advances in Modeling Earth Systems*, 12(5), e2019MS001938. <https://doi.org/10.1029/2019MS001938>
- Zampieri, L., Goessling, H. F., & Jung, T. (2019). Predictability of Antarctic Sea Ice edge on subseasonal time scales. *Geophysical Research Letters*, 46(16), 9719–9727. <https://doi.org/10.1029/2019GL084096>
- Zhang, L., Ren, X., Wang, C.-Y., Gan, B., Wu, L., & Cai, W. (2024). An observational study on the interactions between storm tracks and sea ice in the Southern Hemisphere. *Climate Dynamics*, 62(1), 17–36. <https://doi.org/10.1007/s00382-023-06894-5>
- Zuo, H., Balmaseda, M. A., Tietsche, S., Mogensen, K., & Mayer, M. (2019). The ECMWF operational ensemble reanalysis–analysis system for ocean and sea ice: A description of the system and evaluation. *Ocean Science*, 15(3), 779–808. <https://doi.org/10.5194/os-15-779-2019>